International Journal of Thermophysics, Vol. 25, No. 4, July 2004 (© 2004)

Surface Tension and Viscosity of Succinonitrile–Acetone Alloys Using Surface Light Scattering Spectrometer[1]

P. Tin[2,3] and H. C. de Groh III[4]

Using a surface light scattering spectroscopic technique, the surface tension and viscosity of pure succinonitrile (SCN) and SCN–acetone alloys at 0.86, 1.69, and 2.25 mol% have been determined. The surface light scattering technique, and the procedures used for making the alloys and measuring their concentrations, are presented. Analysis indicates our interfacial surface tension and viscosity measurements have an uncertainty of ±2% and ±10%, respectively. The surface tension and viscosity were measured at various temperatures yielding relations among surface tension, viscosity, temperature, and concentration in SCN–acetone alloys.

KEY WORDS: interfacial surface energy; metal analog; succinonitrile; surface light scattering spectrometer; surface tension; viscosity.

1. INTRODUCTION

Succinonitrile (SCN) and its alloys with acetone (ACE) are widely used metal analogs in experimental and associated numerical studies of solidification with major heat, solute, and fluid transfer components [1–7]. The SCN is optically transparent, has a body-centered cubic crystal structure, a low melting point, and a slightly anisotropic solid/liquid surface tension, γ_{sl}, and thus solidifies dendritically as most metals do. The surface tension and viscosity are important physical properties needed in the analysis

[1]Paper presented at the Fifteenth Symposium on Thermophysical Properties, June 22–27, 2003, Boulder, Colorado, U.S.A.

[2]National Center for Microgravity Research, NASA Glenn Research Center, Cleveland, Ohio 44135, U.S.A.

[3]To whom correspondence should be addressed. E-mail: padetha.tin@grc.nasa.gov

[4]NASA Glenn Research Center, Mail Stop 105-1, Cleveland, Ohio 44135, U.S.A.

0195-928X/04/0700-1143/0

of many aspects of solidification, nucleation, Oswald ripening, and surface tension driven convection (Marangoni convection). Unlike natural convection, which is driven by density gradients within the bulk fluid, Marangoni convection is driven by surface tension forces brought about by temperature and/or concentration gradients (thermocapillary and solutocapillary convection, respectively) along vapor/liquid surfaces. Marangoni convection brought about by the presence of voids and/or bubbles and can drastically change transport processes in solidifying melts, as was shown in recent experiments done on NASAs space shuttle [8–10] and by numerical studies of Kassemi et al. [11–16]. Accurate viscosity and liquid/vapor surface tension, γ_{lv}, data at various temperatures and concentrations are needed to analytically, numerically, and experimentally model solidification and the related governing transport processes; such data for the *model* material SCN alloyed with ACE (SCN–ACE) are presented in this paper.

The surface tension of pure SCN at various temperatures can be found in the literature [17–21]. The authors are not aware of publication of any viscosity or surface tension γ_{lv} data for alloys of SCN. Determination of the surface tension and viscosity can be made non-invasively from the characteristics of light scattered from capillary waves generated by thermally excited surface ripplons [22–24]. The use of surface light scattering (SLS) spectroscopy to measure γ_{lv} and viscosity in SCN is discussed in Tin et al. [17] and Frate [21]. The uncertainty of this technique is $\pm 2\%$ for surface tension and about ± 10 % for viscosity. Using this technique, we have measured the surface tension and viscosity of pure SCN and SCN–ACE alloys at 0.86, 1.69, and 2.25 mol%.

2. EXPERIMENTAL PROCEDURES

2.1. Preparation of Succinonitrile and SCN-Acetone Alloys

Figure 1 shows schematically the placement of the cell, containing the SCN alloy, in the SLS spectrometer. The glass cells had a vertical cylindrical section with optically flat windows at each end, and a feed/riser tube and tee to a graduated cylinder separated by a Teflon stopcock. A thermocouple sleeve through the side of the cell enabled temperature sensors to be placed inside the cell. Type K thermocouples were used for control in the furnace/control/heater loop, and thermistors were used to measure the SCN temperature. The test cell was cleaned and dried with heat under vacuum; high purity (99.9+%) HPLC grade ACE was then put in the graduated cylinder and the stopcock closed. Cells were then connected to the SCN supply container, and the assembly was evacuated. While maintaining vacuum, the SCN was melted using a heat gun; it then flowed by

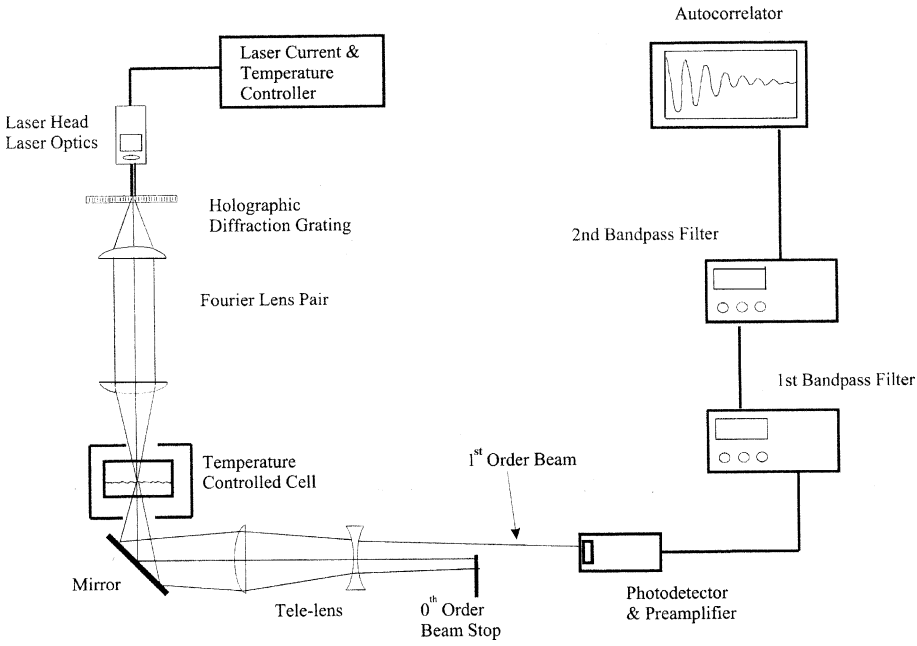

Fig. 1. Schematic of surface light scattering spectrometer (transmission type).

gravity into the cell. The SCN solidified and the upper section of the feed tube was fused closed, sealing the cell under vacuum.

SCN with a measured minimum purity of 99.95% was used. The purity of the SCN was measured by comparing its melting point to that of a Standard Reference Material 1970 SCN triple point standard from National Institute of Standards and Technology (NIST) [25]. The triple point temperature of SCN provided by the NIST standard is 58.0642°C. Melting points were measured using thermistors supplied by Thermometrics Inc. with equation constants optimized for use near 58°C, through NIST traceable calibrations at 37, 58, and 90°C. These thermistors were then calibrated again with the electronics at NASA Glenn using the SCN triple point standard. For these measurements a computer equipped with a National Instruments NI 4351 series high-precision temperature logger was used, enabling resolution to 10^{-4} K. After calibration, thermistor uncertainty was ±0.003°C. The initial solidification temperature, T_o, of the undoped SCN in the cell was determined as in Chopra [26], by monitoring the calibrated thermistor in the cell, placing the cell in a bath, then adjusting the bath temperature so that only a very small amount of solid is

stable while the rest remains liquid. The purity was estimated by assuming a melting point change per mole percent impurity of 2°C/mol%; thus, % impurity = $(T_o - 58.0642°C)/(2°C/mol\%)$. Alloys were made by opening the stopcock and allowing some of the acetone to enter the main section of the cell. The SCN was melted and mixed with the acetone, then the new T_o measured as in Chopra [26]. The concentration of the alloy was then found by dividing the difference between the melting point of pure SCN and T_o ($T_o - 58.0642°C$) by the slope of the SCN-ACE liquidus (2.17°C/mol%) [27].

In general, this paper presents interfacial energies and viscosities as a function of temperature and concentration. The temperature measurements used to determine concentrations had an estimated uncertainty of ±0.003°C. The temperatures measured during SLS used a different set of electronics and did not benefit from a second calibration with the SCN triple point standard, thus had an estimated uncertainty of ±0.01°C. The uncertainty of the concentration measurements is dominated by the uncertainty in the SCN–ACE liquidus slope. A reasonable estimate of the uncertainty of the liquidus slope from the literature is (for concentrations below 7 mol%) $m_l = 2.17 \pm 0.03$ K/mol%. This ±0.03 uncertainty dictates our concentration measurements to have an estimated uncertainty of about ±1.5% (±0.015 mol% at 1%; ±0.15 mol% at 10%).

2.2. Determination of Surface Tension and Viscosity Using Surface Light Scattering Spectroscopy

The determination of the surface tension and viscosity can be made from the non-invasive measurement of the coherent light scattered from capillary waves generated by thermally excited surface ripplons. The theoretical estimate of the amplitude of these surface ripplons is on the order of a tenth of an Angstrom (10^{-11} m) to a few nanometers. The method measures the power spectrum of a narrow selection of the surface waves with frequencies between about 1 and 50 kHz, depending upon the material and temperature. Our SLS system uses the grating heterodyne method (also known as light beating spectroscopy). Härd et al. [28] first developed a similar surface light scattering system consisting of a grating placed in the optical beam path to create a constant local oscillator to beat against the scattered signal. The grating method also selects the scattered k vector, which is an essential factor in the dispersion relation equation when deducing the surface tension and viscosity. Figure 1 shows a schematic of our transmission type SLS spectrometer.

The laser used was a 532 nm frequency doubled Nd:YVO_4 DPSS laser with power stability better than 1%. The beam was broadened and colli-

mated with a telescopic beam expander to a 4 mm diameter beam waist measured at the liquid–vapor interface. The optically heterodyned signal from the first-order diffracted beam is detected by a Si photodetector, amplified, filtered and finally processed in the autocorrelator or a spectrum analyzer. Signal amplification and bandpass filtering was done using two cascaded bandpass filters (EG&G Model 5113) before it was processed by a Brookhaven analogue correlator. The power spectrum, $P(\omega)$, of the ripplons for a given **k** vector is contained in the photodetector current measurement and is approximately given by the Lorentzian relation,

$$P(\omega) = a_0 \left[\frac{\Gamma}{\Gamma^2 + (\omega - \omega_0)^2} + \frac{\Gamma}{\Gamma^2 + (\omega + \omega_0)^2} \right], \tag{1}$$

where ω_o is the center frequency, Γ is the full width at half height, and a_o is a scaling factor constant.

In short, the center frequency, ω_o, and the full width at half height, Γ, are related to the surface tension and kinematic viscosity through the dispersion relation. The dispersion of the ripplon scattering is theoretically given by [29]

$$(\omega_0 + 2\nu k^2)^2 + (\sigma/\rho)k^3 = 4\nu^2 k^4 (1 + \omega_0/\nu k^2)^{1/2} \tag{2}$$

and for low scattering wave number ($k < \sigma\rho\nu^2$), the above equation can be approximated by [30]

$$\omega_o(k) = \frac{\gamma}{\rho}^{1/2} |k|^{3/2}, \quad \Gamma = 2|k|^2 \nu, \tag{3}$$

where ρ is the density of the liquid, ν is the kinematic viscosity ($\nu = \nu_d/\rho$ where ν_d is the dynamic viscosity), **k** is the wave vector, $k = 2\pi/a$, and a is the grating constant.

The spectrum given in Eq. (1) corresponds to the correlation function $R(\tau)$ in the following relationship to the center frequency and half width half maximum of the Lorentzian.

$$R(\tau) = A + B\cos(\omega_0 \tau) e^{-\Gamma\tau}, \tag{4}$$

where A and B are constants. Equation (4) corresponds to the measurements where there is no instrumental broadening due to the finite number of scattering **k** vectors collected into the photodetector, since imaging of the grating onto the surface has finite width. This broadening effect is smallest at the largest **k** vector, but a large **k** vector yields less intensity

that may lead to errors due to poor statistics in the data. Thus, avoiding the instrumental broadening effect by measuring at higher **k** vectors is not an appropriate solution. In our measurements we use low **k** numbers of $250\,\mathrm{cm}^{-1}$. This results in good quality data and complies with the approximation of Eq. (3). In most situations the broadening effect is small enough to be theoretically embedded in the fitting of the function as the convolution of the Lorentzian spectrum and Gaussian profile assuming that the laser beam has the transverse Gaussian mode. Thus, a rigorous approach has been included in the computational procedure of obtaining the corrected center frequency ω_o and Γ. Initially the correlation function data is fitted using the weighted nonlinear least-squares routine to Eq. (4). The resulting parameters are then corrected for the propagation errors and instrumental function that takes into account the instrumental broadening. In the process, it includes the correction of the apparent width of the projected Gaussian beam on the interface. Further details of this numerical method can be found in Ref. 31.

Additional theory and background details regarding SLS can be found in Ref. 17; and since the spectrometer setup and γ_{lv} and ν measurement details also appear in Ref. 17, they are only briefly summarized here. The beam illuminated a diffraction grating with a grating constant of $250\,\mathrm{cm}^{-1}$ developed by Riso National Laboratory, and a diffraction efficiency between 0.5 and 10% for first-order beams. First-order beams heterodyned with scattered light are directed into the photodetector, the signal is then amplified, filtered, and passed to the autocorrelator. Correlation functions at different temperatures were analyzed with a software written in APL code that performs a correlation function fit and computation procedures as explained above to obtain the corrected center frequency, ω_o, and the full width half maximum Γ of the Lorentzian, then the surface tension and viscosity were calculated using Eq. (3). Measurements were done to determine experimental uncertainties using water, acetone, and ethyl alcohol; measurement uncertainty was found to be less than $\pm 2\%$ for surface tension, and $\pm 10\%$ for viscosity [17, 32].

3. RESULTS AND DISCUSSION

3.1. Surface Tension and Viscosity Measurement

Table I contains the surface tension and viscosity measurements of the different alloys at temperatures between 60 and 110°C. Figures 2 and 3 present γ_v and ν_d at the different concentrations and temperatures examined. Analysis of these data results in the following relations of surface tension and viscosity with temperature (T in °C) at various SCN–ACE

Table I. SLS Surface Tensions and Viscosities of Pure SCN and SCN–ACE Alloys at Different Temperatures

Concentration (mol% ACE)	Temperature (°C)	Surface tension ($mN \cdot m^{-1}$)	Viscosity ($mPa \cdot s$)
2.25	60	33.78	1.44
	70	33.26	1.30
	80	32.69	1.22
	90	31.80	0.81
	100	31.66	0.95
	110	30.57	0.71
1.69	60	34.78	1.82
	70	34.21	1.63
	80	33.43	1.45
	90	32.68	1.28
	100	31.92	1.05
	110	31.64	
0.86	60	35.8	2.36
	70	35.09	1.96
	85	34.02	1.50
	90	33.95	1.42
	100	33.2	1.13
	110	32.29	
Pure SCN	60	38.18	2.66
	70	37.32	2.23
	80	36.48	2.01
	90	36.01	1.83
	100	34.89	1.50
	110	33.97	

alloy concentrations (in mol% ACE). For the surface tension (in $mN \cdot m^{-1}$) dependence on temperature at various concentrations

$$\gamma_{(\text{pure SCN})} = 43.14 - 0.0823T \quad (R^2 = 0.9916), \tag{5}$$

$$\gamma_{(0.86\,\text{mol\%})} = 39.88 - 0.0678T \quad (R^2 = 0.9914), \tag{6}$$

$$\gamma_{(1.69\,\text{mol\%})} = 38.77 - 0.0666T \quad (R^2 = 0.9880), \tag{7}$$

$$\gamma_{(2.25\,\text{mol\%})} = 37.57 - 0.0621T \quad (R^2 = 0.9762), \tag{8}$$

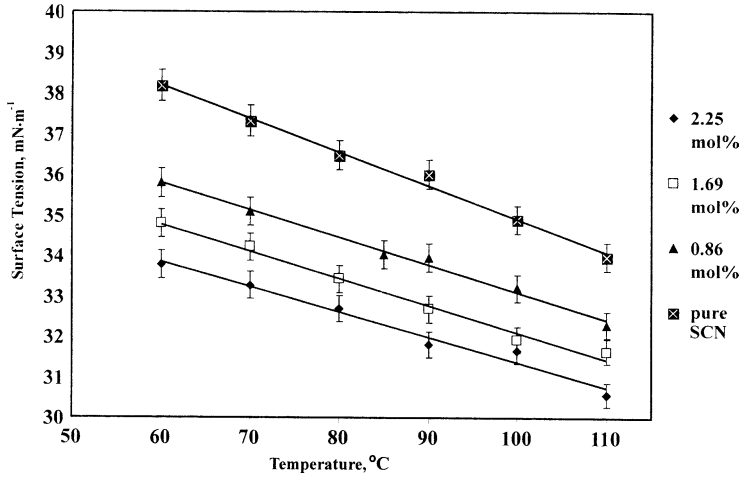

Fig. 2. Surface tension of liquid SCN versus temperature at different concentrations (mol% ACE).

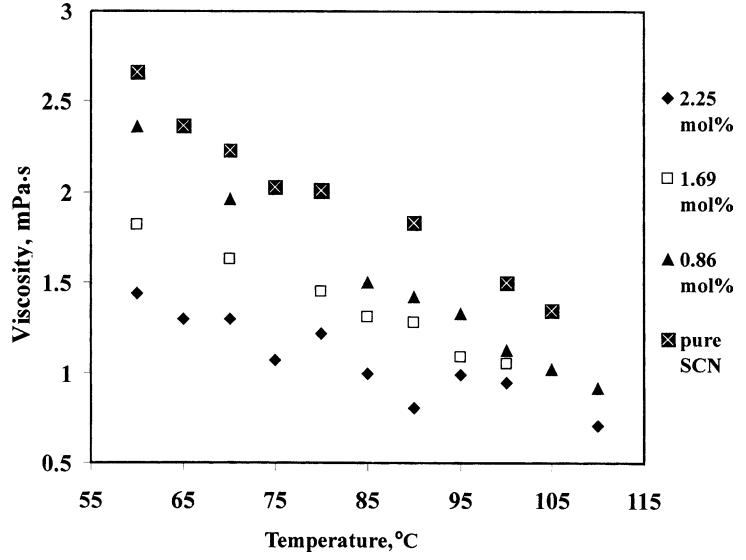

Fig. 3. Viscosity of liquid SCN versus temperature at different concentrations (mol% ACE).

where R is the coefficient of correlation [33]. Also, for the viscosity (in mPa · s) dependence on temperature at various concentrations

$$\nu_{\mathrm{d(pure\ SCN)}} = 4.11 - 0.0263T \quad (R^2 = 0.9715), \tag{9}$$

$$\nu_{d(0.86\,mol\%)} = 3.98 - 0.0283T\,(R^2 = 0.9893), \tag{10}$$

$$\nu_{d(1.69\,mol\%)} = 3.01 - 0.0197T\,(R^2 = 0.9889) \tag{11}$$

$$\nu_{d(2.25\,mol\%)} = 2.18 - 0.0133T\,(R^2 = 0.8411). \tag{12}$$

In an effort to produce a relation with more utility, a linear dependence between surface tension and concentration was adopted; this facilitated the combining of Eqs. (5)–(8) into the following relation among surface tension, concentration (c in mol%), and temperature:

$$\gamma(T, c) = 42.7 - 2.37\ c - [0.080 - 0.0083\ c]T. \tag{13}$$

A linear relation adopted between viscosity and concentration yields the following equation among viscosity, concentration, and temperature

$$\nu_d(T, c) = 4.36 - 0.87\ c - [0.029 - 0.00606\ c]T. \tag{14}$$

Even with the approximating assumption of γ_{lv} and ν_d linearity with concentration, Eqs. (13) and (14) were found to be within the estimated experimental uncertainty of $\pm 2\%$ for surface tension and $\pm 10\%$ for viscosity. Equations (13) and (14) can be used, for example, to estimate the characteristic flow driven by thermo and solutal-capillary forces brought about by temperature and concentrations gradients along a liquid–vapor surface.

4. CONCLUSIONS

Using the surface light scattering spectroscopic technique, we have determined the surface tension and viscosity of pure SCN and SCN–ACE alloys at 0.86, 1.69, and 2.25 mol% ACE. The procedures presented for making SCN–ACE alloys and measuring the initial concentrations (c) and solidification temperatures (T_o) were successful; T_o measurements had an uncertainty of about $\pm 0.005^\circ$C, and concentration measurements had an uncertainty of about ± 0.05 mol%. Based on previous work, comparisons with standards, and analysis of current measurements, our measurements of the interfacial surface tension of SCN–ACE alloys have an estimated uncertainty of $\pm 2\%$, and viscosity measurements have an uncertainty of $\pm 10\%$. The surface tension and viscosity of the alloys were measured at various temperatures, between 60 and 110°C, yielding relations among surface tension, viscosity, temperature, and concentration in SCN–ACE

alloys. These relations are presented in Eq. (13) and (14). Even with the simplifying assumption of linearity between concentration and surface tension (and between concentration and viscosity) Eqs. (13) and (14) appear accurate to within the uncertainties of the experiments (2% for γ_{lv}, 10% for ν_d). It is hoped that these data will provide needed physical property values to those using SCN. Future work will include measuring the surface tension and viscosity of SCN–ACE alloys at higher concentrations of acetone, preferably up to about 10 mol%.

ACKNOWLEDGMENTS

We thank Prof. J. A. Mann, Case Western Reserve University, for assistance and SLS software and Dr. Mohammad Kassemi, The National Center for Microgravity Research, for insights on the needs of the numerical modeling community. This research was funded by NASA Office of Biological & Physical Research, Fundamental Microgravity Research in Physical Sciences (Materials).

REFERENCES

1. G. H. Yeoh, G. de Vahl Davis, E. Leonardi, H. C. de Groh III, and M. Yao, *J. Crystal Growth* **173**:492 (1997).
2. C. Beckermann, H. C. de Groh III, I. Steinbach, and B. T. Murray, *Equiaxed Dendritic Solidification Experiment (EDSE)*, NASA Conf. Publ. 3342, compiled by F. Szofran, D. McCauley, and C. Walker (1996), pp. 137–142.
3. M. E. Glicksman, K. B. Koss, J. C. LaCombe, and A. O Lupulescu, *The Isothermal Dendritic Growth Experiment (IDGE): USMP-4 One-Year-Report*, NASA/CP-1999-209628, compiled by E.C. Ethridge, P.A. Curreri, and D.E. McCauley (1999), pp. 9–16.
4. J. E. Simpson, H. C. de Groh III, and S. V. Garimella, *Directional Solidification of Pure Succinonitrile and a Succinonitrile-Acetone Alloy*, NASA/TM-2000-209381/REV1 (2000).
5. J. E. Simpson, S. V. Garimella, and H. C. de Groh III, *J. Thermophy. Heat Trans* . **16**:324 (2002).
6. B. Q. Li, Y. Shu, K. Li, and H. C. de Groh III, *Fluid Flow and Solidification Under Combined Action of Magnetic Fields and Microgravity*, TMS 2003 Annual Meeting, Session on Mat. Proc. in Elec. and Mag. Fields; also submitted to *J. Mat. Manufac. Proc*.
7. S. Barsi, *The Effects of Void-Induced Thermocapillary Convection on Heat and Mass Transport during Microgravity Solidification*, M.S. Thesis (Case Western Reserve Univ., Cleveland, Ohio, 2003).
8. D. H. Matheson and J. A. Majewski, *The Study of Dopant Segregation Behavior During the Growth of GaAs in Microgravity*, in Joint Launch + One Year Review of USML-1 and USMP-1, NASA CP 3272, Vol. 1 (May 1994), p. 223.
9. J. B. Andrews, L. J. Hayes, Y. Arikawa, and S. R. Coriell, *Microgravity Solidification of Al-In Alloys*, AIAA Paper 97-1012, 35th AIAA Aero. Sci. Meeting (1997).

10. A. L. Fripp, W. J. Debnam, G. A. Woodell, W. R. Rosch, and R. Narayanan, *The Effect of Microgravity Direction on the Growth of PbSnTe*, AIAA Paper 97-0676, 35th AIAA Aero. Sci. Meeting (1997).
11. M. Kassemi and N. Rashidnia, *Steady and Oscillatory Thermocapillary Flows Generated by a Bubble in 1-G and Low-G Environments*, AIAA Paper 97-0924,The 35th AIAA Aero. Sci. Meeting (1997).
12. M. Kassemi and N. Rashidnia, *Oscillatory and Steady Thermocapillary and Natural Convective Flows Generated by a Bubble: Numerical-Experimental Comparisons*, Proc. Joint Xth Europ. and Russ Symp. Phys. Sci. in Microgravity, V. S. Avdyevsky and V. I. Polezhaev, eds., Vol I (1997), pp. 110–117.
13. M. Kassemi, N. Rashidnia, and C. Mercer, *Numerical and Experimental Visualization of Oscillatory Temperature and Velocity Fields Generated by a Bubble*, Proc. 8th Int. Symp. in Flow Visualization, G. M. Carlomagno and I. Grant, eds. (1998), pp. 284.1–284.11.
14. M. Kassemi and N. Rashidnia, *Phys. Fluids* **12**:3133 (2000).
15. M. Kassemi, M. Kaforey, and D. Matthiesen, *J. Thermophy. Heat Transfer* **15**:219 (2001).
16. M. Kassemi, S. Barsi, M. Kaforey, and D. Matthiesen, *J. Crystal Growth* **225**:516 (2001).
17. P. Tin, D. Frate, and H. C. de Groh III, *Int. J. Thermophys*. **22**:557 (2001).
18. J. A. Dean, *Lange's Handbook of Chemistry* (McGraw-Hill, New York, 1985).
19. J. Jasper, *J. Phys. Chem. Ref. Data* **1**:841 (1972).
20. P. Walden, *J. Phys. Chem*. **75**:555 (1911).
21. D. Frate, M.S. Thesis (Case Western Reserve University, Cleveland, Ohio, 1998).
22. R. H. Katyl and U. Ingaard, *Phys. Rev. Lett*. **19**:64 (1967).
23. R. H. Katyl and U. Ingaard, *Phys. Rev. Lett*. **20**:248 (1968).
24. D. Langevin, *Light Scattering by Liquid Surfaces and Complementary Techniques*, Vol. **41**, Surface Science Series (Marcel Dekker, New York, 1992).
25. B. W. Mangum and Samir El-Sabban, *SRM 1970: Succinonitrile Triple-Point Standard – A Temperature Reference Standard Near 58.08°C*, NBS Spec. Pub. 260-101 (1986).
26. M. A. Chopra, *Influence of Diffusion and Convective Transport on Dendritic Growth in Dilute Alloys,* Ph.D. Thesis (Rensselaer Polytechnic Institute, Troy, New York, 1983).
27. M. A. Chopra, M. E. Glicksman, and N. B. Singh, *Met. Trans A*. **19A**: 3087 (1988).
28. S. Härd, Y. Hamnerius, and O. Nilsson, *J. Appl. Phys* . **47**:2433 (1976).
29. L. Kramer, *J. Chem.Phys*. **55**: 2097 (1971).
30. V. G. Levich, *Physicochemical Hydrodynamics* (Prentice Hall, Englewood Cliffs, New Jersey, 1962), p. 603.
31. R. V. Edwards, R. S. Sirohi, J. A. Mann, L. B. Shih, and L. Lading, *Applied Optics* **21**:3555 (1982).
32. P. Tin, J. A. Mann, W. V. Meyer, and T. W. Taylor, *Appl. Phys*. **36**:7601 (1997).
33. J. E. Freund, *Modern Elementary Statistics*, 5th Ed. (Prentice-Hall, Englewood Cliffs, New Jersey, 1979), p. 394.